Proceedings of the 2009 IEEE
International Conference on Robotics and Biomimetics
December 19 -23, 2009, Guilin, China

Signal Processing and Fabrication of a Biomimetic Tactile Sensor Array with Thermal, Force and Microvibration Modalities

Chia Hsien Lin, Todd W. Erickson, Jeremy A. Fishel, *Student Member IEEE*,
Nicholas Wettels, *Student Member IEEE* and Gerald E. Loeb, *Senior Member IEEE*

***Abstract*— We have developed a finger-shaped sensor array that provides simultaneous information about the contact forces, microvibrations and thermal fluxes induced by contact with external objects. In this paper, we describe a microprocessor-based signal conditioning and digitizing system for these sensing modalities and its embodiment on a flex-circuit that facilitates efficient assembly of the entire system via injection molding. Thermal energy from the embedded electronics is used to heat the finger above ambient temperature, similar to the biological finger. This enables the material properties of contacted objects to be inferred from thermal transients measured by a thermistor in the sensor array. Combining sensor modalities provides synergistic benefits. For example, the contact forces for exploratory movements can be calibrated so that thermal and microvibration data can be interpreted more definitively.**

I. Introduction

Tactile feedback is essential for dexterous use of the hand. Physical therapists working to rehabilitate hands with neurological damage understand that tactile sensation is a key indicator of ultimate hand function. Information from mechanical and thermal receptors in the skin is used constantly both to provide conscious awareness of objects and their attributes for motor planning and to make subconscious motor adjustments to stabilize contact with the objects according to general goals specified by the brain. It is difficult to imagine much progress in the design of mechatronic prostheses or robots until they are provided with sensory transducers that can support such functions.

A. Multimodal Sensor Concept

In the biological hand, mechanical forces, vibrations, and temperature are detected by specialized receptors that are distributed throughout the skin and pulp of the fingertip. Wettels et al. (2008) have described a fingertip with similar mechanical structure and novel sensors of skin deformation that provide wide dynamic range sensing of normal and shear forces [1]. Electrodes distributed on the surface of the rigid core respond to deformations of the skin by changing their electrical impedance through a weakly conductive fluid that is compressed between the skin and core (See Fig. 1). Fishel et al. (2008) demonstrated that microvibrations associated with slip and texture could be extracted from sound waves that propagate from the skin, through the fluid and into a conventional pressure transducer in the core, whose high-pass filtered signal is essentially that of a hydrophone [2]. Here we describe the addition of a thermistor to measure temperature and heat fluxes associated with the material properties of contacted objects. All sensing elements and associated signal conditioning electronics are mounted on a printed flex-circuit that is molded into the rigid core of a finger. This core is covered with a polymeric skin, fluid (mechanically equivalent to pulp) and rigid nail elements that are mechanically and cosmetically similar to biological fingers. These BioTAC™ modules (Fig. 1) will be integrated mechanically, electronically and functionally into a variety of prosthetic and robotic hands intended to provide function for patients with loss of normal hand function as a result of trauma and disease.

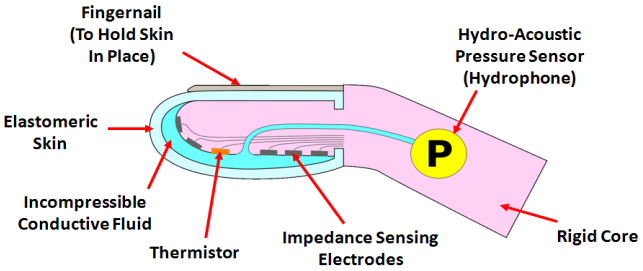

Fig. 1. Schematic diagram of the BioTAC™ biomimetic tactile sensor. Sensing modalities include: measurement of normal and shear forces detected by changes in impedance between electrodes as fluid pathways deform [1], detection of slip related microvibrations which propagate through the skin and fluid and are detected by the hydro-acoustic pressure senor [2], and thermal properties as detected by a thermistor capable of detecting heat flow between the preheated core and contacted objects.

B. Synergistic Signal Processing

Force, vibration, and thermal information collected by the BioTAC™ during various contact tasks have many synergistic relationships, so a sensor capable of detecting all of these properties is necessary for extracting useful information. For example, vibrotactile signals are affected by the normal force between the skin and the object over which it is sliding. In the BioTAC™, the normal force must be extracted from changes in the conductance of the fluid

Manuscript received July 31, 2009. This work was supported by Award Number R43HD061165 to SynTouch LLC from the Eunice Kennedy Shriver National Institute Of Child Health & Human Development. The content is solely the responsibility of the authors and does not necessarily represent the official views of the Eunice Kennedy Shriver National Institute Of Child Health & Human Development or the National Institutes of Health.

Chia Hsien Lin is with Syntouch LLC, Los Angeles, CA 90007 USA (phone: 626-512-1579; e-mail: gary.lin@syntouchllc.com)

Todd Erickson (e-mail: twericks@usc.edu) and Gerald Loeb (email: gloeb@usc.edu) are with the Dept. of Biomedical Engineering, University of Southern California, Los Angeles, CA 20089 USA.

Jeremy Fishel (email: jfishel@usc.edu) and Nicholas Wettels (email: nick.wettels@syntouchllc.com) are with SynTouch LLC and the University of Southern California.

978-1-4244-4775-6/09/$25.00 ©

between electrodes, whose conductivity is strongly dependent on temperature. The core can be heated above the ambient temperature so that contact with an external object induces thermal fluxes that depend on the thermal properties and size of the object. These temperature changes can be measured by a thermistor on or near the surface of the core, but they depend also on the location of the location and surface area of the contact, which depends also on the contact force. Thus, the various modalities of data from one or more tactile sensors must be transmitted at a sufficiently high rate to a central controller where the data can be considered in light of voluntary command signals and the state of the actuators.

II. Background

Several exotic technologies have been applied to the thermal sensing problem in haptics: fiber Bragg gratings [3], carbon nanotubes [4] and MEMS embodiments yielding skin-like configurations [5, 6]. Others groups use more traditional devices like thermistors, but also use them in conjunction with force sensors and heating elements in the sensors [7, 8] when applied to grippers. When a heated end-effector contacts an object at room temperature, this generates a dynamic temperature changes according to the geometry and thermal properties of the object and end-effector. As the amount of force between them increases, the skin deforms around the object, increasing the contact area between them. This increase in contact area will cause an increase in heat transfer between the objects.

Humans discriminate objects thermally using a similar mechanism [9]. Skin contains afferents that respond not only to absolute temperature, but to temporal gradients as well. Experiments by Jones and Berris [10] have shown that human subjects are able to discriminate objects more reliably based on their heat capacity rather than their thermal conductivity (within 5 – 8 seconds) but the discrimination of objects based on their thermal properties at room temperature is relatively coarse in normal human subjects [10, 11].

The strategy to replicate heat-flow sensing for object discrimination is not new. This same strategy was used with the Utah-MIT Hand developers [12], by Monkman with Peltier devices [13] and more recently by Engel *et al.* and Takamuku *et al*. using strain sensors, heating elements and temperature detectors to track thermal and force profiles of contacted objects [14, 15]. The aforementioned devices, however, require a large number of wired and/ or delicate surfaces that are probably insufficiently rugged for field use. Also, many of these analyses do not extend beyond features of the DC temperature profile of the sensor. The authors posit that there may be many discriminable features in the AC temperature domain. Our goal is to produce a device that can discriminate objects thermally as well as or better than human subjects [8]. Surveys of tactile sensing can be found in [16-19].

III. Methods

A. Integrated Signal Processing

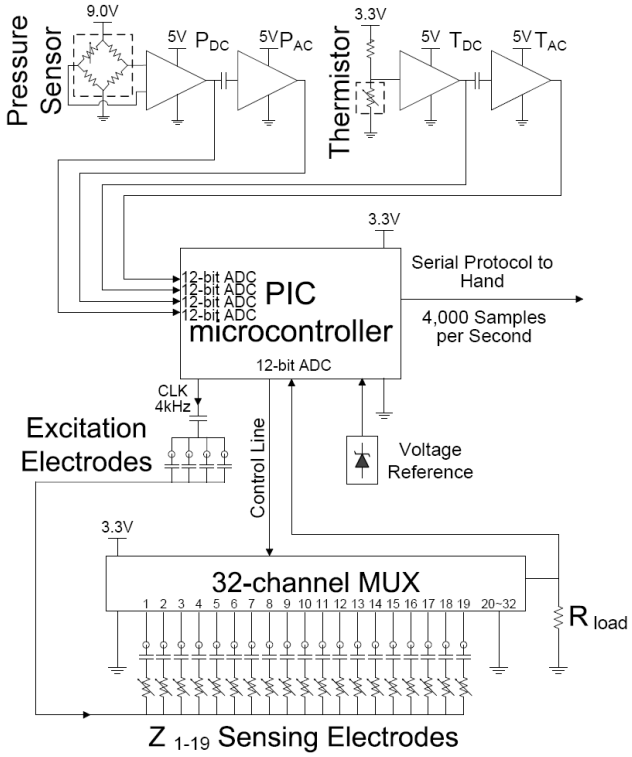

Fig. 2. BioTAC™ flex-circuit electronics. This circuit provides the signal processing needed for output via serial protocol to a prosthetic hand. Similar circuitry with a 16-channel MUX (Analog Devices Inc., #ADG758) has been built and validated on a conventional printed circuit board before the miniaturization shown in Fig. 3.

The complete signal processing chain is illustrated schematically in Fig. 2. It is embodied in a miniature 3-layer flex-circuit (Figs. 3 – 5) that carries all sensing electrodes, transducers and electronic components for placement in the mold that forms the rigid core. The impedance sensing electrodes are switched by multiplexer (Analog Devices, Inc., #ADG732) and connected in turn to R_{load} and the internal analog-to-digital converter in the PIC microcontroller (Microchip Technology Inc., #dsPIC33FJ128GP802). This circuitry measures the peak voltage produced by the current passing through the fluid path from the excitation electrodes – several similar contacts distributed around the fingertip and driven by an AC-coupled, 4kHz clock that is synchronous with the multiplexer (MUX) and ADC operations. The off-the-shelf MEMS pressure sensor (Honeywell, #26PC15SMT) is a resistive bridge that is amplified by operational amplifiers (Analog Devices, Inc., #AD8630) to produce both DC (pressure) and AC (vibration) signals. The off-the-shelf thermistor (GE, #EC95) is similarly amplified to provide both DC (absolute temperature) and AC (thermal flux) signals. A single frame consists of sampling all available Z-channels plus P_{DC}, T_{DC} and T_{AC}, interleaved with frequent sampling of P_{AC} to provide 1kHz bandwidth for the vibration signals. Several frames of data are buffered and

transmitted via Serial Protocol Interface (SPI) bus every 10ms upon request from a master PC or other controller. Data were transmitted (National Instruments, USB-8451 with LabVIEW 8.0) and analyzed offline (MathWorks, MATLAB). Sample output signals from a printed circuit board (PCB) version are described below (see Fig. 8).

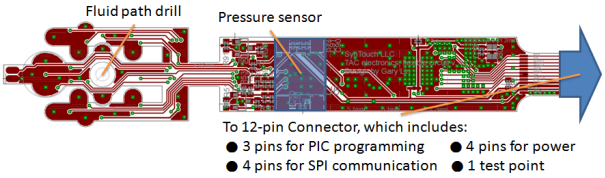

Fig. 3. Top layer of flex-circuit layout. The pressure sensor (vibration modality) is located on this layer. The solder pads for the thermistor are at the tip on the left.

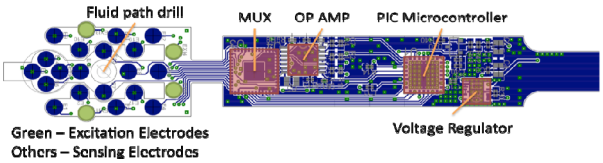

Fig. 4. Bottom layer of flex-circuit layout. The blue and green sensing and excitation electrodes are for the impedance (force) modality. Note the green vias near the PIC Microcontroller and Voltage Regulator are thermal vias which help to distribute the generated heat more quickly through the entire BioTAC™. The multiplexer (MUX) and operational amplifier (OP AMP), PIC microcontroller, and the voltage regulator (National Semiconductor Inc., # LP2986) are all located on this layer.

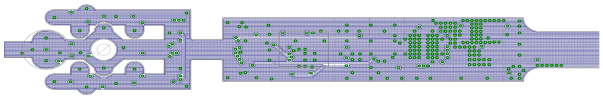

Fig. 5. Middle layer of Flex Circuit: ground layer. The complex outline of the flex-circuit at the left end is designed to facilitate contact of all the sensing electrodes with the curved bottom of the mold used to form the rigid core in which this flex-circuit is embedded.

B. Heat Source

The PIC microcontroller heats the device to the desired temperature by adjusting the clock frequency of the PIC microcontroller according to feedback from the thermistor. The electronic circuitry generates between 125 and 250 mW of power. While the sensor is touching an object, force-impedance sensors gather information to analyze the contact forces and shape of the object. At the same time, the PIC microcontroller gathers thermistor information and analyzes object thermal properties.

Conventional thermistors mounted on the core will tend to respond slowly to contact with hot or cold objects because the fluid and skin will impede heat flux. A fast time constant is not needed because thermal environments are not expected to change quickly nor is the goal to provide rapid thermal feedback to prevent damage to the skin, which has a high operating range and is easily replaced. Power dissipation energy from the other components is comparatively small and can be ignored.

C. Heat-Flow Sensation

A prototype approximating the thermal generation and sensing components of the BioTAC™ was used to demonstrate the feasibility of using heat-flow sensing via a thermistor to discriminate objects. The sensor consisted of two 40-Ohm resistors (heaters) in the back section and three thermistors (GE EC95, Type F): two monitoring the temperature of the heaters and a third in the tip for thermal characterization of contacted objects. These electronic components were placed into a mold and cast with an epoxy-based encapsulant (Stycast 1264) to generate a core with the size and shape of the BioTAC™. The core was covered with a molded silicone elastomer skin and inflated with approximately 1cc of propylene glycol as used in the BioTAC™. The two heaters were powered with a 5V source providing 1.3W of power. After powering and reaching equilibrium, the sensor's temperature was approximately 85°C at the heaters and 31°C in the tip (ambient 25°C).

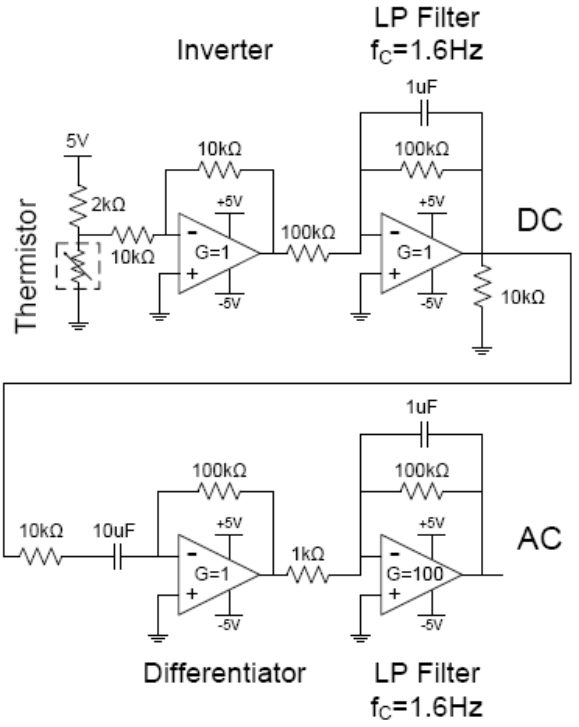

Fig. 6. Signal processing for thermal experiments.

Voltage was measured via voltage divider, analogue low-pass filtered (1.6 Hz) and recorded by a custom LabVIEW program. The signal was differentiated and amplified to enhance AC transients (Fig. 6).

The sensor was mounted to a pivot on the stepper motor's base, allowing the finger to contact the sample material consistently. The sample was placed on an insulating piece of foam mounted on the force plate (Advanced Mechanical Technology, Inc., Model HE6X6-16). The stepper motor (Nippon Pulse America, Inc., PFL35T-48Q4C (120) stepper motor, NPAD10BF chopper drive) was used to press the tip of the finger against the sample material with a force of 10N (Fig. 7). Copper, Aluminum, Stainless Steel and Plastic were tested; Table 1 provides density, heat capacity, thermal conductivity and thermal diffusivity. Each material was

machined into a thick puck (101mm diam x 25mm thick; effectively infinite heat sink relative to sensor mass) and a thin puck (0.8mm thick) to test the effect of heat capacity. Each puck was tested three times.

TABLE 1
Test Samples and Thermal Properties

Material	Density (kg/m^3)	Heat Cap (J/kgK)	Conductivity (W/mK)	Diffusivity (m^2/s)
Cu	8890	385	388	1.13E-04
Al	2810	960	130	4.82E-05
Steel	7750	460	17.9	5.02E-06
Plastic	953	1850	0.4	2.269E-07

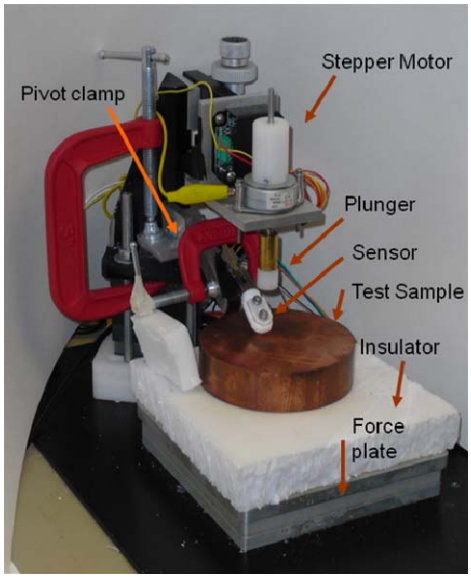

Fig. 7. Thermal Test Assembly

The digitized voltages were converted to their corresponding temperatures and temperature derivatives using MATLAB. As expected, the temperature profile (after initial transients described below) had the form of an exponential decay with the time constant and equilibrium temperature being dependent on the object being contacted. The following equations were used for positive and negative temperature exponentials (1) and derivatives (2):

$$T(t) = T_f + (T_0 - T_f) \exp(-t/\tau) \quad (1)$$

$$T(t) = T_f - (1/\tau)(T_0 - T_f) \exp(-t/\tau) \quad (2)$$

Analyzing the above equation at t=0 the following equation is true:

$$T(0) = -\tau \, dT(0)/dt + T_f \quad (3)$$

Using this relation, the temperature response was plotted against its derivative, and a linear fit was applied to obtain the time constant τ, and the steady state value T_f.

IV. Results

A. Electronics

The multiplexed analog data are digitized every 250µs by the internal 12-bit ADC in the PIC (4 kHz sampling rate). Measurements of the vibrations P_{AC} at 2 kSamples/s are interleaved with the electrode impedances (Z_n) and other sensor signals. Thus, the frame of sampling consists of 32 data words representing P_{AC}, Z_1, P_{AC}, Z_2, …, P_{AC}, Z_{13}, P_{AC}, P_{DC}, P_{AC}, T_{AC}, P_{AC}, and T_{DC}. The PIC microcontroller rearranges these data in a transmission buffer with sequencing: $Z_{1\text{-}13}$ impedance samples, 16 P_{AC} samples (vibration), P_{DC} (pressure), T_{AC} (thermal flux) and T_{DC} (absolute temperature).

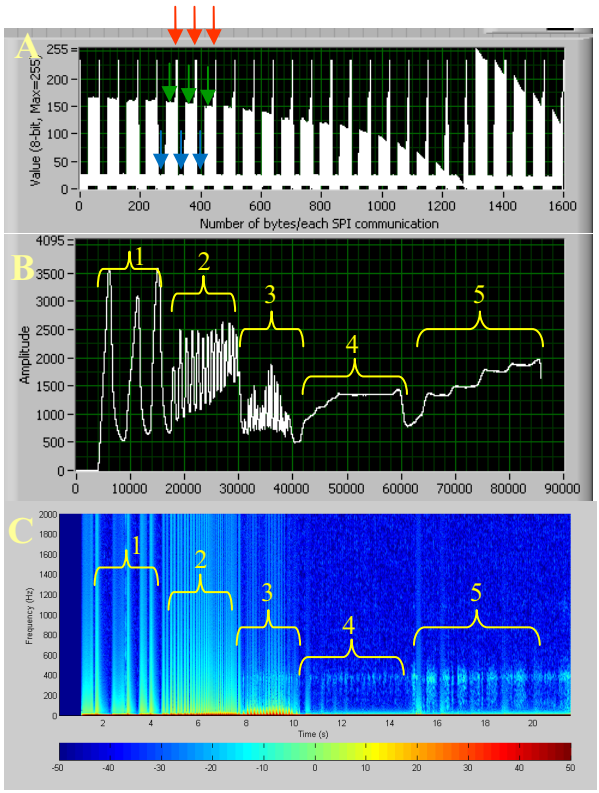

Fig. 8. Data collected from the prototype PCB. A) The raw data from the SPI bus for a short period (approximately 400 msec) consisting of 25 communications (1600 bytes of data transmission). B) Extracted pressure data for 5 sequential operations (brackets, see text), about 90,000 samples. C) MATLAB power spectrum analysis. Stimuli 3-5 have dominant energy near 400 Hz (tested on a skin with smooth rather than fingerprint textured external surface).

Because the SPI is constricted by NI USB-8451 that can only transmit byte-width (8-bit) data, the PIC microcontroller splits every data word into two data bytes and organizes them into a 64-byte array plus header and tail bytes for transmission through SPI bus. The equal-spaced peaks (orange arrows in Fig. 8A) denote a tail of one array followed by a header of the next array. The samples following the peaks represent impedance values (blue arrows), vibration (green arrows), pressure, thermal flux, and absolute temperature. During this experiment only the pressure was varied, thus only the P_{AC} data are fluctuating. Five different

fluid pressure stimuli (brackets in Fig. 8B: 1 slow push-pull, 2 fast push-pull, 3 vibration, 4 sliding lightly over a rough surface, and 5 sliding over a rough surface with larger downward force) were applied via syringe to the pressure sensor during this data collection. Consecutive 66-byte data buffers were imported by LabVIEW, which converted them into calibrated decimal values for display as continuous waveforms. Figure 8C illustrates the Short Time Fourier Transform (STFT) analysis in MATLAB.

B. Thermal Analysis

Upon contact with a test object, the derivative of temperature (T_{AC}) has several reproducible features. The initial negative peak rate of change is similar for all materials because this cooling effect is due to the somewhat cooler skin first contacting the thermistor (Fig. 9 below). The skin surrounding the sensor is closer to ambient temperature than the core because of the intervening fluid and proximity to ambient air.

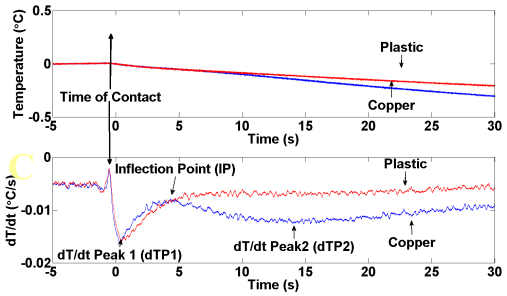

Fig. 9. T_{DC} (top) and T_{AC} (bottom) following contact (vertical arrows) with large plastic and copper test pucks.

After the initial transient, features of the contacted object emerge. The next notable feature is an inflection point in the rate of temperature change. Following contact with plastic, T_{AC} reverts to a gradually decreasing rate of cooling. During contact with copper, cooling is faster and exhibits a second negative peak. Similar behavior can be seen for the other metal samples (Fig. 10).

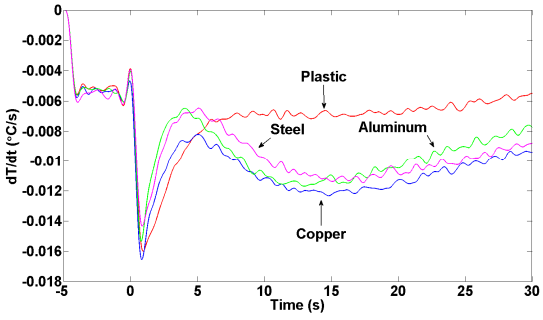

Fig. 10. AC transient responses for large tests samples: digitally filtered with 1 Hz Butterworth LPF for clarity.

A summary of extracted features and respective times is proved in Tables 2A and 2B:

TABLE 2A

Landmark features extracted from T_{AC} data

	dT/dt Peak 1		Inflection Point	
Material	**Time (s)**	**dTdt (°C/s)**	**Time (s)**	**dTdt (°C/s)**
Copper	0.8	-0.021	4.8	-0.010
Aluminum	0.7	-0.016	3.8	-0.006
Steel	0.9	-0.020	5.2	-0.006
Plastic	0.9	-0.019	6.9	-0.005

TABLE 2B

Landmark features continued, time constant is extracted from T_{DC}.

	dT/dt Peak 2		Time Constant
Material	**Time (s)**	**dTdt (°C/s)**	**(s)**
Copper	13.5	-0.013	43.1
Aluminum	12.6	-0.012	41.1
Steel	12.7	-0.011	49.4
Plastic	6.9	-0.005	55.3

Comparing the thin versus thick samples, the change in mass seems mostly to affect the magnitude of the derivative, and not the timing of its features. The inflection point was moved to an earlier time for all materials. The time constants for the thin samples were significantly less than the time constants of the corresponding thick samples (Table 3). The value for the thin plastic sample was too small for accurate determination in light of the slow negative drift at the beginning of all runs (Fig. 11).

TABLE 3A

Changes in landmark features for thin samples

	dT/dt Peak 1		Inflection Point	
Material	**Time (s)**	**dTdt (°C/s)**	**Time (s)**	**dTdt (°C/s)**
Copper	0.4	-0.0114	-2.2	-0.0004
Aluminum	0.6	-0.0109	-1.3	-0.0001
Steel	0.3	-0.0101	-3.2	-0.0006
Plastic	0.1	-0.0152	-4.9	-0.0003

TABLE 3B

Changes in thin features (continued)

	dT/dt Peak 2		Time Constant
Material	**Time (s)**	**dTdt (°C/s)**	**(s)**
Copper	-0.9	-0.0119	20.6
Aluminum	0.0	-0.0140	23.4
Steel	-0.1	-0.0108	23.8
Plastic	-4.9	-0.0003	13.3*

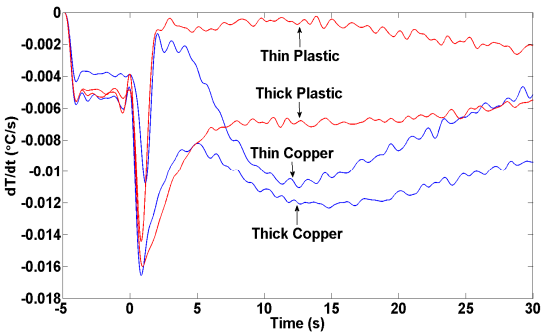

Fig. 11. T_{AC} transients for thick vs. thin samples.

V. Discussion

A. Electronics

The PIC microcontroller successfully supports all three sensing modalities and also meets the critical space requirement. The PIC microcontroller and the voltage regulator can serve as heat sources to heat the finger up to the desired temperature for thermal flux sensing. It can also be readily reprogrammed to support different communication protocols such as I^2C and USB. Some of the data sources appear to have sufficiently low noise to warrant 16-bit digitization, which is readily achieved at these low sampling rates by adding an external ADC.

B. Extraction of Thermal Properties

The thermal processes underlying the temperature transients upon contact are non-linear and complex, but simple linear approximations that can be computed on-line may well be sufficient to identify general material classes. For the limited range of materials and volumes tested to date, the timing and magnitude of Peak 2 appear to be reasonably correlated with specific heat capacity (R^2 = 0.69-0.93) and thermal bulk (R^2 = 0.59-0.84). This is in agreement with the psychophysical discriminability reported by Jones and Berris [10] in humans, perhaps based on similar mechanisms. As the object remains in contact with the sensor, it absorbs progressively more heat from the sensor, which is continuously heated from an internal source (electrical power dissipation in the BioTAC™; blood supply in the human). The cooling rate will pass through a peak whose time and magnitude is determined by the time constants of the thermal resistive and capacitive properties of the sensor and the object. For the conditions of test reported here, total thermal capacity appears to be the dominant factor.

For actual use in the field, the thermal data must be deconvolved with other information about the geometry of the object, the location of the point of contact with respect to the thermistor, and the deformation of the skin around the object, which determines the contact area. Information about all of these features can be extracted from the array of impedance sensing electrodes. It is not clear, however, whether an analytical solution is possible or even necessary. In order to match the relatively coarse discriminability achieved by humans, it may be sufficient to compare the extracted features of the thermal data to a reference table of contact events collected empirically from known objects.

REFERENCES

[1] N. Wettels, V.J. Santos, R. Johansson, and G.E. Loeb, "Biomimetic tactile sensor array." Advanced Robotics, vol. 22, no. 7, pp. 829-849 June 2008

[2] J.A Fishel, V.J Santos, Loeb G.E., "A Robust Micro-Vibration Sensor for Biomimetic Fingertips," *Proc. of International Conference on Biomedical Robotics and Biomechatronics,* Scottsdale, Arizona, *In press*, 2008

[3] J.S. Heo and J.J. Lee, "Temperature Sensor Array for Tactile Sensation Using FBG Sensors" in *Proc of 5th IEEE Conference on Sensors*, pp. 1464-1467 Daegu, South Korea 2006

[4] Selvarasah et al. "A Three-dimensional thermal sensor based on single walled carbon nanotubes." 14th International Conference on Solid-State Sensors, Actuators and Microsystems pp. 1023-1026, Lyon, France, June 2007

[5] Y.J. Yang *et al*. "A wireless flexible temperature and tactile sensing array for robot applications" in Proc. Of Fourth International Symposium on Precision Mechanical Measurements, December 2008

[6] T. Someya *et al,* "Conformable, flexible, large-area networks ofpressure and thermal sensors with organic transistor active matrixes" PNAS vol. 102 no. 35 pp. 2321–12325 August 2005

[7] K. Shida K. and J. Yuji, "Thermal-type tactile sensor for material discrimination and contact pressure sensing" In Proc of 41st Annual SICE Conference vol.1 pp.588- 589 August 2002

[8] R.A. Russell, "A thermal sensor array to provide tactile feedback for robots" *Int'l Journal of Robotics Research* Vol. 4 No.5 Fall 1985

[9] D.C. Spray "Cutaneous Temperature Receptors," *Ann. Rev. Physiol. 48:625-38* 1986

[10] L.A Jones and M. Berris, "Material Discrimination and Thermal Perception" *Proc. of the11th Symposium on Haptic Interfaces for Virtual Environment and Teleoperator Systems* pp. 137-142, 2003

[11] W.M. Bergmann Tiest, "An experimentally verified model of the perceived 'coldness' of objects" In *Proceedings of the 2nd joint Eurohaptics conference and Symposium on haptic interfaces and teleoperator systems* (pp. 61–65). 2007

[12] J. M. Hollerbach, D. Siegel, I. Garabieta, "An Integrated Tactile and Thermal Sensor" *Proc of 1986 IEEE International Conference on Robotics and Automation* pp. 1286 - 1291 April 1986

[13] G. J. Monkman and P. M. Taylor, "Thermal Tactile Sensing" IEEE Trans. Robotics & Automation vol. 9, pp. 313 – 318, June 1993

[14] Engel *et al.* "Flexible Multimodal Tactile Sensing System for Object Identification" Proc of IEEE EXCO SENSORS, Daegu, South Korea, October 2006

[15] S. Takamuku, T. Iwase and K. Hosoda, "Robust material discrimination by a soft anthropomorphic finger with tactile and thermal sense" in *Proc from IROS* pp. 3977-3982 September 2008

[16] R.D Howe, "Tactile Sensing and Control of Robotic Manipulation," in *Journal of Advanced Robotics*, Vol.8,No.3, pp. 245-261, 1994

[17] M. H. Lee and H. R. Nichols, "Tactile sensing for mechatronics—a state of the art survey," *Mechatronics* 9, pp.1–31, 1999

[18] C. Melchiorri, "Tactile Sensing for Robotic Manipulation," *Ramsete: Lecture Notes in Control and Information Sciences* Vol. 270 Springer Berlin, 2001

[19] V. Maheshwari and R. Saraf, "Tactile Devices To Sense Touch on a Par with a Human Finger" Angew. Chem. Int. Ed., 47, pp. 7808 – 7826, 2008